RAM.

**ROBOTICS
AND
MECHATRONICS**

A SENSOR FUSION TECHNIQUE FOR HEAD MOTION CONTROLLED ENDOSCOPE CAMERA SYSTEM

V. (Vineeth) Panambur Venkatraman

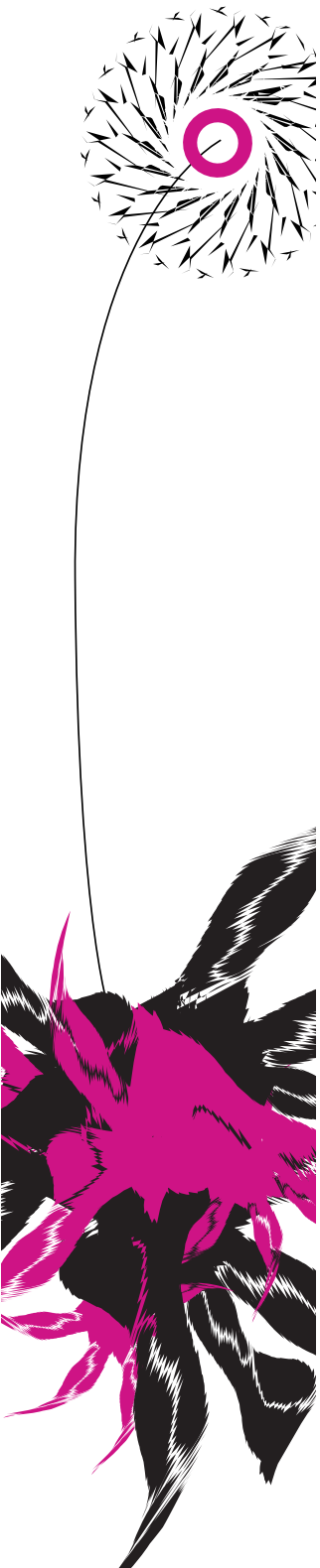MSC ASSIGNMENT

Committee:
dr. ir. M. Abayazid
Y.X. Mak, MSc
dr. ir. F. Heijden
dr. S.U. Yavuz

November, 2019

UNIVERSITY OF TWENTE. | TECHMED CENTRE   UNIVERSITY OF TWENTE. | DIGITAL SOCIETY INSTITUTE

Summary

Video assisted thoracic surgery (VATS) is a type of minimally invasive surgery (MIS) in which the movement of the endoscope camera is done by assistant of an surgeon. A head motion controlled endoscope system was developed to enable the surgeon to directly control the endoscope using his/her head motion. The image output obtained from the endoscope was displayed on the screen. A compensation of the image rotation is done to remove the rotation component in the motion of the output image. This is done to keep the directionality in the image same as the head movement of the user. The compensation was done using the angle of rotation of the servo encoder measurement at the image plane and the angle of rotation obtained from optical flow based estimation. However, the image rotation compensation of the image output was not accurate because the output obtained from optical flow based estimation was suffering from drift and the output obtained from the servo encoder measurement was not accurate in finer motions.

During this master's assignment, a sensor fusion technique for obtaining a better image rotation compensation and compensating for non-linearities in the actuation of the head motion controlled endoscope camera system has been developed and evaluated. The rotation obtained from the servo encoder measurement and the rotation obtained from the optical flow based estimation on the image output is fused together. Complementary filter and Extended kalman filter (EKF) were the two sensor fusion algorithms used. The complete software implementation was done in ROS Kinetic.

Human trials were conducted to evaluate the performance of the head motion controlled endoscope camera system after compensating for image rotation. The accuracy test suggested that EKF was comparitively better sensor fusion algorithm and the test for compensating hysteresis behavior suggested that Complementary filter was relatively better sensor fusion algorithm. From the response of human trials for overall performance of the system, it was observed that the complementary filter was preferred over EKF and servo encoder measurements. These results obtained from this study prove that sensor fusion algorithms can be used for improving the performance of the head motion controlled endoscope camera system.

Acknowledgements

First and foremost, I would like to thank my parents for their unconditional love and support throughout my study here in University of Twente. I would like to thank my little sister also for her daily dose of rant. Without their support, I would not have been in this position right now.

I would like to express sincere gratitude to dr.ir.Momen Abayazid for giving me this opportunity to work on this project, broadening my view in field of clinical research and to work with clinicians, surgeons during this master's assignment. He has been a patient mentor, providing guidance during my learning process in research. I would like to thank my daily supervisor, Yoeko Mak for his assistance, feedback and mostly for bearing with me asking silly doubts everytime. He has helped me with the approach of critical thinking required to solve a problem. This has helped a lot, well during the end of the research. I would like to thank dr.ir.Ferdi van der Heijden for his feedback during this project and also for being the chair of the graduation committee, and dr. S.U.Yavuz for being the external member of the graduation committee. I want to thank our collaborator from Universitair Medisch Centrum Groningen (UMCG), notably Maurits Zegel and prof dr. Massino Mariani for their support.

The time spent in RaM lab was fun, working together with other master students. I would like to thank Husain, Antonio, Shrijan, Atul, Sanlap for accompanying inside the lab and outside the lab for a coffee or sharing knowledge. I would like to thank all the members of the RaM department, especially medical robotics group for their support. Special thanks to Jolanda for her love and support during those phases of stress and panic. I would like to thank all the technicians, colleagues for their support. To all my friends in enschede, thank you so much. You all are a part of my small family in Netherlands. To all my friends in wageningen, thank you so much. It's time to hit Krishna Vilas for a plate of Paneer chilly.

Finally, I would like to thank my beloved partner Vishaka for her love and support. Without those weekends spent together eating and chilling, it would have been difficult.

Also to my second home, Netherlands you were amazing except for the weather. If you are reading this thesis, thank you very much and please enjoy.

Vineeth Panambur Venkatraman
Enschede, 01-11-2019

Contents

1 Introduction

1.1 Context

Video Assisted Thoracic Surgery (VATS) or also called Thoracoscopic surgery has been performed widely over recent decades. These surgeries are performed for treating common diseases such as Lung cancer, Emphysema etc. Since this surgery is one of the types of minimally invasive surgery (MIS), the advantages are decreased postoperative pain and faster recovery, with short hospital stay. During this surgery, small incisions are made through which the special surgical instruments and the endoscope, which provides the visuals of the operative area are inserted. The visuals are transmitted to the monitor stationed near the patient for the surgeon's visual feedback.
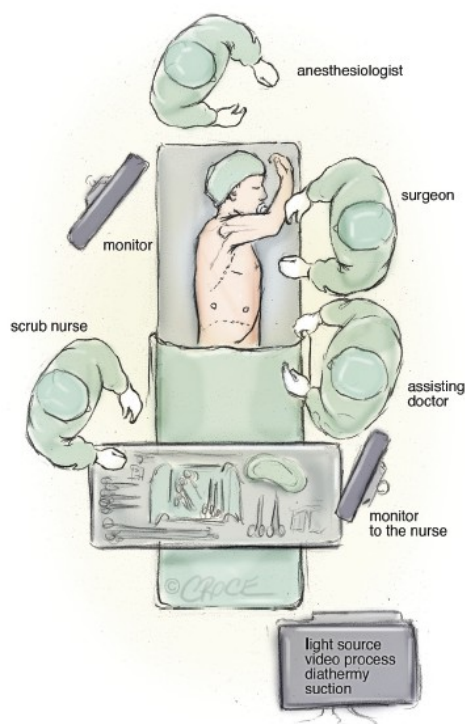

Figure 1.1: Setup of the operating room during the VAT surgery, from Hansen and Petersen (2012).

The surgery often requires a camera assistant to hold and control the thoracoscope, while the surgeon is performing the operation, shown in the figure 1.1. However, there are some limitiations related to visual-feedback system during VATS surgery in general and they are discussed below:

- The assistant controls the endoscopic camera, which creates a limiting factor because the control of the endoscopic camera is completely dependent on the communication between the surgeon and the assistant.

- The movement of the endoscope is limited inside the patient's body such that the endoscope should not interfere with other surgical instruments or exert excessive pressure on the incisions made.

- The space during VAT surgery is limited due to many people and surgeons are needed to work in such a relatively small space. Normally the surgery requires a lot of medical personnel to perform, hence the surgeon and the assistant may not have a direct look at the monitor, which leads to stress and fatigue during long operations.

- The post-surgery recovery is needed due to the pain experienced by the patient. This is due to the pressure applied at the incisions during the surgery using the rigid endoscope system which is currently used.

Several robotic systems solutions such as AESOP (Sackier and Wang (1994)) which was controlled by voice, PMASS (Minor et al. (2008)) which was controlled by body etc. have been presented to control the endoscopic cameras more efficiently. These systems reduced the use of an assistant during the surgery.

In this study, we focus on the head motion controlled endoscope system. Reilink et al. (2010) presented a head-motion controlled gastroscope. This work contained the design and system-level implementation of a flexible gastroscope, with a head mounted display for visual output. Another relevant work presented by Mak (2018) contains the design of a head-motion controlled endoscope system, where the endoscope was controlled by surgeon's head movement and the image was displayed on the monitor. The flexible endoscope that was used in this work was Ambu aScope 3 Regular. The work also presented the clinical evaluation and solution to the problem that is mentioned above.

1.2 Problem Statement

A compensation of the image rotation is done to remove the rotation component in the motion of the output image. This is done to keep the directionality in the image same as the head movement of the user. The image rotation compensation stabilizes the output rotation. The hysteresis observed in the system are due to thumb lever control of the endoscope and backlash in the actuation mechanism. However, there were some issues that were observed corresponding to image rotation compensation and hysteresis compensation. They are:

- The compensation was done by two ways. Firstly, the image rotation was obtained from the angle of rotation of servo encoder measurement and secondly the rotation was obtained from the image data using SimpleFlow optical flow algorithm. However, the results obtained from the servo motor was not accurate in the finer motion due to non-linearities present in the cable and the results that were obtained from the image output were suffering from drift over a period of time (Mak (2018)).

- The hysteresis was plotted based on just the deflection angle of the servo motor.

- The Ambu aScope version was upgraded from 3 to 4. Due to the upgrade, the robot handle that was designed in the previous work could not hold the new endoscope.

In this study, we will look into sensor fusion approach for improving the image rotation compensation and hysteresis compensation. A work presented by Selman (2017) contains a sensor fusion algorithm between an Computer-Vision-based device and an inertial motion capture system. Gui et al. (2015) presented a comparison between complementary filter and kalman filter for IMU data fusion. A highly relevant work presented by Raghavan (2016) contains a sensor fusion algorithm for Human motion estimation. This was done by obtaining the data from the camera and the IMU. The data were validated by statistical analysis. From this, we can now define our research goal.

1.3   Research Goal

From the problems that were observed from the previous work, we can propose a research question to meet the requirements for current project:

How can we improve the performance of the image rotation compensation and remove non-linearities in the actuation of the head motion controlled endoscope system?

To address the main research questions, sub-questions were formed:

RG1 Can a sensor fusion technique be used for improving the accuracy of the image rotation compensation?

RG2 How can we compensate for the non-linearities in the actuation of the motor by the image data?

RG3 Can a sensor fusion technique be used for improving the human performance on the overall system?

An engineering problem was also stated below:

EP How can we fit the new design of the Ambu aScope to the existing model?

The head-scope system which was already used for the previous work will be used for this project as well. The servo and the image data are fused together and is compared with ground truth. The data is validated using statistical analysis. The fused data will be used for displaying the image output on the screen. The complete system will then be tested with human trials, for assessing the performance of the overall system.

1.4   Report Outline

This master thesis is outlined as follow:

- This chapter (Chapter 1) presents a general description of the assignment, problem statement and the research objectives.

- The developed sensor fusion technique and the human trails conducted for measuring the performance are summarized in paper format explained in Chapter 2. A brief explanation of the sensor fusion algorithms and the design changes that were made to the system (**EP**) are summarized in this chapter. The results are also discussed and the main research question is addressed (**RG1**, **RG2** & **RG3**).

- Chapter 3 presents the conclusion, limitations and future work.

- The instructions manual and the questionnaire form of the human trial experiment are presented in Appendix [A].

2 Paper: A Sensor Fusion Technique for Head Motion Controlled Endoscope Camera System

In the current video assisted thoracic surgery (VATS), the assistant of an surgeon controls the movement of the endoscopic camera. A head motion controlled endoscope system was developed enabling the surgeon to control the endoscope directly using his/her head motion. The image output obtained from the endoscope was displayed on the screen. A compensation of the image rotation is done to remove the rotation component in the motion of the output image. This is done to keep the directionality in the image same as the head movement of the user. The compensation was done using the angle of rotation of the servo encoder measurement at the image plane and the angle of rotation obtained from optical flow based estimation. However, the image rotation compensation for the image output was not accurate because the output obtained from optical flow based estimation was suffering from drift and the output obtained from servo motor was not accurate in finer motions. In this paper, we propose a sensor fusion technique for obtaining a better image rotation compensation for the head motion controlled endoscope camera system. The rotation obtained from the servo motor and the rotation obtained from the optical flow based estimated on the image output will be fused together. Complementary filter and the Extended Kalman Filter (EKF) are the two sensor fusion algorithms used in this study. The complete software implementation was done on ROS Kinetic. Human trials were conducted for evaluating the performance of the overall system after compensating for image rotation. Results indicate that the Complementary filter was relatively better sensor fusion algorithm compared to the Extended Kalman filter.

A Sensor Fusion Technique for Head Motion Controlled Endoscope Camera System

Vineeth Panambur Venkatraman[1] Yoeko Mak[1] and Momen Abayazid[1]

Abstract— In the current video assisted thoracic surgery (VATS), the assistant of an surgeon controls the movement of the endoscopic camera. A head motion controlled endoscope system was developed enabling the surgeon to control the endoscope directly using his/her head motion. The image output obtained from the endoscope was displayed on the screen. A compensation of the image rotation is done to remove the rotation component in the motion of the output image. This is done to keep the directionality in the image same as the head movement of the user. The compensation was done using the angle of rotation of the servo encoder measurement at the image plane and the angle of rotation obtained from optical flow based estimation. However, the image rotation compensation for the image output was not accurate because the output obtained from optical flow based estimation was suffering from drift and the output obtained from servo motor was not accurate in finer motion.

In this paper, we propose a sensor fusion technique for obtaining a better image rotation compensation for the head motion controlled endoscope camera system. The rotation obtained from the servo motor and the rotation obtained from the optical flow based estimation on the image output will be fused together. Complementary filter and the Extended Kalman Filter (EKF) are the two sensor fusion algorithms used in this study. The complete software implementation was done on ROS Kinetic.

Human trials were conducted for evaluating the performance of the overall system after compensating for image rotation. Results indicate that the Complementary filter was relatively better sensor fusion algorithm compared to the Extended Kalman filter.

Keywords–Video Assisted Thoracic Surgery (VATS), Endoscope, Complementary filter, Extended Kalman Filter (EKF), sensor fusion, ROS Kinetic.

I. INTRODUCTION

Video Assisted Thoracic Surgery (VATS) is one of the types of minimally invasive surgery (MIS) for treating common diseases such as Lung cancer, Emphysema etc. They have been performed widely over the recent years. The advantage of MIS is that the post-operative pain for the patients is less compared to the conventional open surgery. During this surgery, three small incisions of size approximately 1 inch each are made in-between the rib cage through which the instruments and a thoracoscope, an endoscopic camera can be passed through [16]. A general overview of the operating room during the VATS surgery is shown in figure 1 below.

[1]V.Panambur Venkatraman, Y.Mak and M.Abayazid are with Faculty of Electrical Engineering, Mathematics and Computer Science, University of Twente, 7522 NB Enschede, The Netherlands `v.panamburvenkatraman@student.utwente.nl`, `y.mak@utwente.nl`, `m.abayazid@utwente.nl`
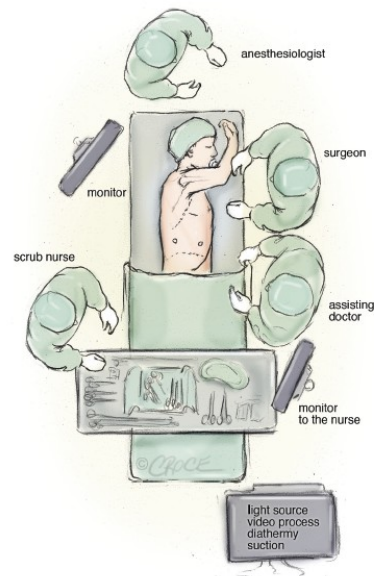
Fig. 1: Operating room setup during VATS surgery. [1]

During the surgery, thoracoscope is passed through the incision allowing the surgeon to get the visuals inside the body. The visuals are transmitted to the monitor stationed near the patient shown in figure 1. The VATS surgery have several limitations related to control and the visual-feedback system. They can be classified into three categories. Firstly the surgery often requires an assistant to hold and steer the thoracoscope, which requires the space in the operating area where the surgeon needs to stand [2]. This results in cramping of position for both the assistant and the surgeon leading to fatigue, stress and unstable view of the monitor shown in figure 2. Secondly, the assistant may not move the thoracoscope exactly as how the surgeon would like. Finally, the movement of the thoracoscope inside the patient's body is limited such that it should not interfere with other instruments. The movement should not exert more pressure on the incisions.

Over the recent years, several robotic systems that can hold the thoracoscope have been developed providing solution for the first and second category of limitations. Systems such as AESOP [3],which is controlled over voice and Freehand [4] allows the surgeon to control the thoracoscope, thus reducing the need of an assistant during the surgery. The use of flexible endoscope such as bronchoscope and gastroscope [6][7] over currently used rigid thoracoscope provides a better solution

Fig. 2: VATS surgery: The assistant (left) holding the thoracoscope between the hands of the surgeon (right) causing constrain in position. [2]

in the movement of the endoscope inside the patient's body during VATS, thus providing a solution for the final category of limitations. Several preceeding work have been done on controlling the endoscopic camera more efficiently. In this paper, we are interested in the robotic systems that have been developed using the head motion as the input source for the control of the endoscope. Reilink et al. [2] developed a head motion controlled gastroscope, where the control of the flexible endoscope was by done by the motion of the head. Previous work done by Mak et al. [5] contains the design of a head-motion controlled endoscope system. The endoscope was controlled by the surgeon's head movement and the image was displayed on the monitor. The flexible endoscope that was used in this work was Ambu® aScope™ 3 regular (Ambu A/S, Copenhagen, Denmark). This work also provided clinical evaluation and solutions to the three categories of limitations that were discussed above.

However, some of the limitations were observed which corresponded to the image rotation compensation and the hysteresis compensation. They are:

- The image rotation output was obtained from the rotation of the servo encoder measurement projected on the image plane and the image output, calculated by SimpleFlow algorithm. The results showed that rotation obtained from the servo motor was not accurate in the finer motion and the rotation obtained from the image was suffering from drift over a period of time. [5]
- The hysteresis was plotted only using the input deflection angle of the servo motor.

There was an upgrade of the endoscope version from Ambu® aScope™ 3 regular to Ambu® aScope™ 4 regular, due to which the robot handle could not hold the new endoscope.

In this paper, we will focus on a sensor fusion approach for obtaining a better image rotation compensation and a better hysteresis compensation. Several works with regard to sensor fusion have been developed. From the work of Selman [8], the IMU data and the data from the Microsoft Hololens were fused. Gui et al. [10] presented a comparison between

complementary filter and kalman filter based on IMU data. One relevant work of Raghavan [9] presented a sensor fusion algorithm for human motion estimation. The validation of the results were done by statistical analysis. Discussing these points above, a research question is defined:

How can we improve the performance of image rotation compensation and remove non-linearitites in the actuation of the head motion controlled endoscope system?

To address the question, sub-questions were also formed:

- Can a sensor fusion technique be used for improving the accuracy of the image rotation compensation?
- How can we compensate for the non-linearities in the actuation of the motor by the image data?
- Can a sensor fusion technique be used for improving the human performance on the overall system?

Also adding to it, an engineering problem was also stated below:

- How can we fit the new design of the Ambu® aScope™ to the existing model?

The paper is organized as follows: Section II provides some basic background knowledge about the head scope modules and the sensor fusion techniques. The design changes that were made for the robot handle are also discussed under this section. The experimental setup for the validation of the sensor fusion technique are also discussed under this section. Section III discusses the results of the experiments that were conducted. Section IV concludes and provides the limitations and possible direction for future work.

II. MATERIALS AND METHODS

This section provides a brief summary of the head scope modules and the two sensor fusion algorithms. The design changes that were made for the robot arm of the system and the experimental setup for reaching our objectives have also been discussed in this section.

A. Head Scope Modules

The general working of the head scope modules is presented in the block diagram shown in figure 3.

The function of each module of the system is explained below:

- The head orientation is measured using XSens MTw Awinda wireless IMU. The IMU is attached to head band or on the Microsoft Hololens.
- The orientation mapper (Servo controller) maps the sensor frame to the camera frame. It also listens to the footswitch signal and then sends the joint positions to the servo motors.
- The advantage of having a footswitch is that it provides the user a control trigger mechanism to either enable or disable the control of the endoscope. This helps the user to freely move their head by releasing the footswitch.
- The endoscope, Ambu® aScope™ 3 regular is then mounted on the Endoscope gripper. The endoscope comes with a monitor, where the analog image output
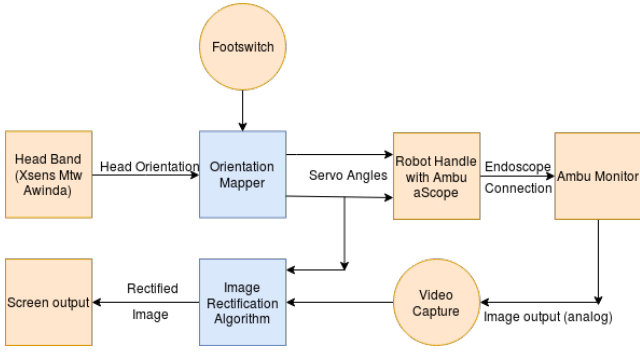
6

Fig. 3: Block diagram of the Head motion controlled endo-scope system. The orange blocks in the figure refer to the physical devices and the blue blocks refer to the software algorithms. [5]

can be transported through the RCA port of the monitor. The image is then captured using the video capture card.
- After the image is captured, image rotation compensation is done to stabilize the output image rotation. This is done by two ways: (1) By projecting the rotation of the servo motor into the image plane. (2) By computer vision algorithms, done on the image itself. They are briefly summarized in the section II-A.1 and II-A.2.
- The compensated image is then visualized either on a monitor or on the Hololens by sending the compressed image output to it.

The two ways by which the image rotation is calculated are explained below [5].

1) Compensation by Servo motor: The rotation obtained from the servo motor is given by the equation (1)

$$\theta = q_1 \cos(q_2) \qquad (1)$$

where q_1 and q_2 are the joint positions of the servo motors [5]. The q_1 and q_2 are obtained from the figure 4 below. q_1 is the rotation around rotation axes actuated by the servo motor and q_2 is the rotation around deflection axes of the servo motor.
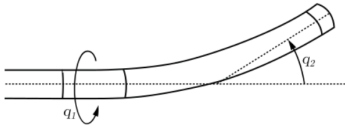

Fig. 4: Illustration of the endoscopic tip, showing the rotation and deflection axes actuated by servo [5].

The image rotation is calculated by

$$R = \begin{bmatrix} \cos(\theta) & -\sin(\theta) \\ \sin(\theta) & \cos(\theta) \end{bmatrix} \qquad t = R \begin{bmatrix} -\frac{w}{2} \\ -\frac{h}{2} \end{bmatrix} + \begin{bmatrix} \frac{w}{2} \\ \frac{h}{2} \end{bmatrix} \qquad (2)$$

where t is translation of the image and w, h are the width and height of the image in pixels. Since the rotation needs to be done around the center of the image, the translation term t is required.

2) Compensation by Image: The rotation obtained from the image, is done by SimpleFlow algorithm. The optical flow algorithm is used to detect the change between two consecutive frames of the image, and the rotation is directly estimated in the image. SimpleFlow algorithm is one of the dense optical flow algorithm which uses all or majority of the pixels from the input image frame. It has low computational cost compared to other dense optical flow algorithms. This algorithm utilizes a color invariance assumption, defining that a same point in a different frame is assumed to have same color vector. The brief explanation of the SimpleFlow algorithm is done in [15]. The output obtained from the algorithm is a 2D flow vector for each pixel in the input image. Using the flow vectors, we estimate the rigid trans-formation. In practical, this transformation is estimated by using estimateAffinePartial2D() from OpenCV library shown in equation 3 below.

$$\begin{bmatrix} \cos(\theta)s & -\sin(\theta)s & t_x \\ \sin(\theta)s & \cos(\theta)s & t_y \end{bmatrix} \begin{bmatrix} x \\ y \\ 1 \end{bmatrix} = \begin{bmatrix} x+u \\ y+v \\ 1 \end{bmatrix} \qquad (3)$$

where (u,v) are the flow vector at the image coordinates (x,y) and s is the scaling factor. The scaling factor enlarges or shrinks the image by a factor. The image is rectified by following the same method as from equation 2, where the scaling factor s and the translation terms t_x and t_y are discarded [5].

B. Design Changes

Ambu® aScope™ 3 endoscope was used for the design and realization of head motion controlled endoscope system [5]. Over the past year, there was an engineering development of endoscope and the new version Ambu® aScope™ 4 came out. The Ambu® aScope™ 3 was outdated. A overview of the Ambu endoscope connected to the robot controller are shown in figure 5. The new Ambu endoscope and the changes in the thumb lever is shown in figure 6 There were few changes made to the new endoscope. The thumb lever pressor of the old robot arm did not fit the new endoscope. Also, the clamper which holds the endoscope on the robot arm did not close properly. Hence the whole handle had to be redesigned. The rest of the parts of the old robot arm were kept the same, including the servo motors.

Fig. 5: Robot controller with Ambu endoscope (left), without the endoscope (center) and Ambu® aScope™ 3 Regular (right) [5]

The new design of the included an increase of the length of clamper by 150 mm. The robot handle was also increased

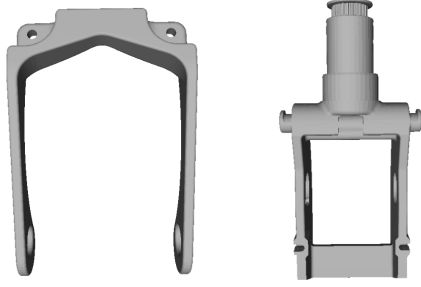Fig. 6: Ambu® aScope™ 4 (left) and the new design of the thumb lever (right)

Fig. 7: New design of the endoscope handler of the robot arm

by a length of 150 mm. The 3D overview of the robot arm is shown in figure 7.

Four hooks were made to hold the thumb lever pressor of the endoscope shown in figure 8. These parts were 3D printed in ABS Material. The new endoscope was then placed inside the new robot handle that was designed. The new design, hence answered one of the sub-questions of the research goals.

Fig. 8: New design of the pressor of the thumb lever of endoscope.

C. Sensor Fusion Algorithms

The two sensor fusion algorithms which are going to be implemented in the system are explained briefly below.

1) Extended Kalman Filter: The extended kalman filter (EKF) is a non linear version of the kalman filter, which linearizes the the current mean and the state covariances that are estimated [12]. The equations of the extended kalman filter in general terms are explained below [11]. Consider a process with a non-linear system, with

$$x_k = f(x_{k-1}) + w_{k-1} \tag{4}$$

where x_k is the state estimate at time k, f is a non-linear state transition function and w_{k-1} is the process noise. In our case $x_k=[\theta_s, \theta_i, \theta]$, where θ_s is the angle of rotation estimated from equation (1) above, θ_i is the angle of rotation estimated from optical flow based estimation and θ is the angle estimated after filtering. The non-linear state transition function is given by equation (5) below:

$$f(x_{k-1}) = f(x_{k-1}^a) + J_f(x_{k-1}^a)e_{k-1} \tag{5}$$

where J_f is the jacobian of f(.) or F and $e_{k-1} = x_{k-1} - x_{k-1}^a$.

The output measurement that is received are in the form of

$$z_k = h(x_k) + v_k \tag{6}$$

where z_k is the output measurement at time k, h is a non-linear function and v_k is the measurement noise. The z_k in this study is the measurement obtained from the servo encoder measurement and the output of optical flow algorithm obtained in terms of angle. The non-linear function h is defined by the function below:

$$h(x_k) = h(x_k^f) + J_h(x_k^f)(x_k - x_k^f) \tag{7}$$

where J_h is the jacobian of h. The jacobian of h or H matrix is shown in equation (8) below.

$$H = \begin{bmatrix} 1 & 0 & 0 \\ 0 & 1 & 0 \end{bmatrix} \tag{8}$$

The prediction step is carried out to project the current state estimate and error covariance forward in time, shown by the equations (9) and (10).

$$x_{k|k-1} = f(x_{k-1}) \tag{9}$$

$$P_{k|k-1} = FP_{k-1}F^T + Q \tag{10}$$

where P is the covariance matrix of the error of the estimates at time $k-1$, F is the jacobian of the function f evaluated at value of x_{k-1} and Q is the assumed covariance matrix of the process noise. To obtain a better motion model that matches the system, the values of the diagonal in the noise covariance matrix must remain small. Equation (4) and equation (10) represent the prediction step (time update). Now that the prediction step is completed, the correction step is then carried out. The Kalman gain K is computed using the equation (11), where K is the Kalman gain, H is the observation matrix or Jacobian of h.

$$K = P_{k|k-1}H^T(HP_{k|k-1}H^T + R)^{-1} \tag{11}$$

$$x_{k|k} = x_{k|k-1} + K(z_k - Hx_{k|k-1}) \qquad (12)$$

The estimate x_k is then updated using the equation (12). The error covariance P is updated by equation (13)

$$P_k = (1 - KH)P_{k|k-1}(1 - KH)^T + KRK^T \qquad (13)$$

where R is the assumed covariance matrix of the measurement error. If the diagonal value is set to a large value, it will result in rapid convergence for initial measurements. Equations (11) to (13) represent the measurement step(Correction step).

The EKF algorithm is implemented from the robot localization package in ROS Kinetic. The robot localization package estimates the position of the robot in a 3D space using non-linear state estimators. The experimental setup of the system to validate the results are explained in the following section II-D.

2) Complementary Filter: The complementary filter is usually used to fuse accelerometer data and gyroscopic data [10]. In our case, the servo angle is assumed as the accelerometer data because the servo can set the bias and we are interested in the high frequency of the servo signal. The change in the image angle per frame is assumed as the gyroscopic data for the integration, since the image data can handle faster dynamics and it drifts over a period of time. The complementary filter simply consists of both low pass filters and high pass filters and it takes advantage of both the servo data and the image data, giving precise output [10]. The block diagram of a complementary filter is shown in figure 9.
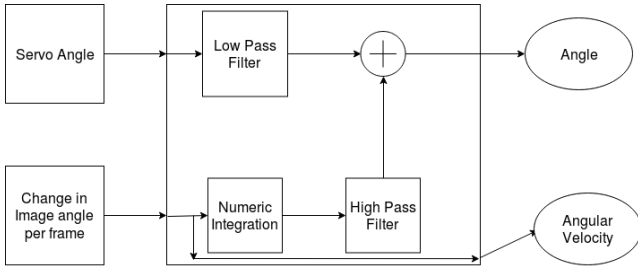

Fig. 9: Block diagram of the Complementary Filter. [10]

With respect to a complementary filter, the time constant τ remains same for both low pass filters and high pass filters. The τ is defined as the boundary between trusting the image data or the servo data. On a short period of time less than τ, the complementary filter uses the image data which is not affected by the external forces and on a long term, it uses the data from the servo to prevent the drift in the system. The angle θ in the complementary filter is calculated by equation (14)[10].

$$\theta = \alpha * (\theta_{k-1} + \omega_{image} * d\tau) + (1 - \alpha) * \theta_{servo} \qquad (14)$$

where α is calculated from the equation (15), θ_{k-1} is the previous angle estimated by complementary filter, ω_{image}

is the change in the angle measured from each frame of the image, and θ_{servo} is the angle measured from the servo motor.

$$\alpha = \frac{\tau}{\tau + d\tau} \qquad (15)$$

where τ is the desired time constant and $d\tau$ is the sample rate of the system. $d\tau$ is calculated by $1/f_s$, where fs is the sampling frequency.

The time constant τ was considered as 25 ms since that is the time one loop of the node takes to complete. The sampling frequency f_s was 28Hz, which was the update rate of each node in ROS Kinetic. Hence, the sample rate $d\tau$ was 0.0375s. After knowing the values of τ and $d\tau$, we now can calculate the α from equation (15). The α was found out to be 0.6 and (1-α) was 0.4. The complementary filter package was developed on ROS Kinetic. The setup for experiments are same as section II-D.

D. Experimental Setup

This section explains in detail the measurement setup for validation of tip movement, image rotation compensation and human trials. These experiments are conducted to answer the main research question and sub-questions. To check for the non-linearities in the actuator of the motor, a hysteresis curve between the servo deflection angle and sensor fusion algorithms was plotted to answer one of the sub-questions of the research mentioned in the section I above. An accuracy test was conducted for image rotation compensation to answer one of the sub-questions of the research. Finally, human trials were conducted to evaluate the performance of the head motion controlled endoscope system after compensating for image rotation, to answer one of the sub-questions of the research and finally to answer the main research question of this study.

The accuracy test was done by statistical analysis. The error was calculated by measuring the data from the sensor fusion algorithms against ground truth signal collected using an electromagnetic based tracking system mounted at the camera position. For evaluating the test, the Root Mean Square Error (RMSE) were used. The RMSE was calculated using the equation 16 below.

$$RMSE = \sqrt{\frac{1}{N} \sum_{k=1}^{N} e_k^2} \qquad (16)$$

Lower the value of RMSE, better is the estimate. A questionnaire was designed to evaluate the overall performance of the system and the human trials were done in a similar manner outlined in this section.

The experimental setup was done by placing an NDI Aurora 6DOF electromagnetic (EM) tracker alongside endoscopic tip, which is integrated to an NDI tabletop system shown in figure 10.

The interface for the head motion controlled endoscope was built in the Robot Operating System (ROS) environment.
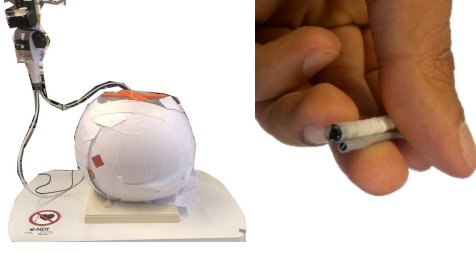
Fig. 10: NDI tabletop system (left). 6DOF EM tracker placed alongside endoscopic tip to obtain the camera pose(right).

The advantages of using ROS is it's flexible software structure, re-usability of the code, easy implementation of communication between different systems and easy integration of different languages and environments of programming.

1) Tip Movement Validation: This was a standalone experiment done by one user. The experimental setup is for conducting this experiment is mentioned above. The validation of the tip movement is done to set the mapping between the servo motor input angle and the real deflection angle at the tip of the endoscope. This is crucial for 2 reasons:

- The movement of the tip of the endoscope inside the body to due to cavity wall may not be equal to the servo deflection angle.
- Presence of non-linear behavior due to the Bowden cable mechanism which is used to move the endoscopic tip.

Two of the parameters are measured in this setup. One is the tip deflection angle q_2 when an input motion is given to the servo motor and another is the angular velocity, which is the change in pixels from the previous frame to the next frame of the image output. These 2 inputs are then fused with the sensor fusion algorithms. For validation, a calculation of hysteresis percentage was done. The points defined for the calculation of percentage are obtained by figure 18 below. In our case for the plot of hysteresis, the x-axis is the tip deflection angle and the y-axis is the output of the sensor fusion algorithms.
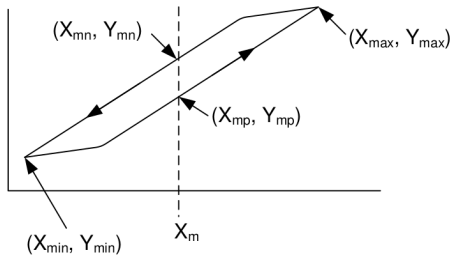

Fig. 11: Definition of points for Hysteresis percentage calculation. [14]

$$X_m = \left(\frac{X_{max} - X_{min}}{2}\right) + X_{min} \qquad (17)$$

where X_m is the midpoint of the curve, X_{max} and X_{min} are the maximum and minimum values of the tip deflection angle. After calculating the midpoint, the two Y values are then calculated as shown in figure 18 above and then the hysteresis percentage is calculated using the equation (18) below.

$$Hysteresis\% = \left|\frac{(Y_{mn} - Y_{mp})}{(Y_{max} - Y_{min})}\right| * 100 \qquad (18)$$

The calculated hysteresis percentage is then compared with the ground truth.

2) Image Rotation Compensation Validation: The image rotation compensation accuracy is measured using the setup mentioned above. This was also a standalone experiment done by one user. The image rotation is obtained by measuring the rotation normal to the camera plane. The rotation angle obtained from the servo motor and the image rotation data explained in the section II-A.1 and II-A.2, are fused with the sensor fusion algorithms and then the data is compared with the ground truth (EM Tracker). Head motion of the user is considered as the source of input for these experiments since it corresponds to the use of the system in a practical case. For the accuracy test of the image rotation compensation, we consider three cases. Case 1 defines the free motion of the head, where the standalone user for the experiment moves his head from the center or the starting point to the left and then to the right reaching the targets of red and green marks shown in figure 12. Case 2 defines the deflection of the tip when the user moves his head from starting point to left and then to the center to up and finally towards right direction reaching red, blue and green marks shown in figure 13. Case 3 is when a data collected by a random motion from left to right and up to down reaching targets of red, blue, green and black mark are merged with the data of the previous cases to check whether the accuracy of the image rotation remains the same for the standalone user. The test was done by statistical analysis mentioned above.
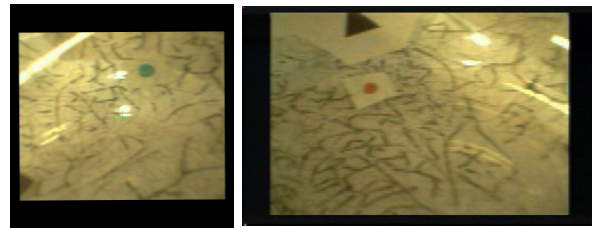

Fig. 12: Screenshot of Green (left) and Red (right) mark inside the dome.

3) Human trials for performance of image rotation compensation: Human trials were conducted for evaluating the performance of the overall system. These trials were conducted because the input head motion might differ from user to user and the user might have a preference of the image output on the screen. However, the performance of the system has to be independent of the user. The setup of the trials
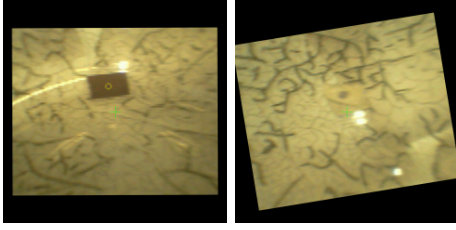
Fig. 13: Screenshot of the Black (left) and Blue (right) mark inside the dome.

were same as the previous standalone experiment conducted. After the trials were over, a questionnaire (Appendix [A]) was carried out with each user to get a qualitative analysis on the preference of the sensor fusion algorithms for better performance of the system.
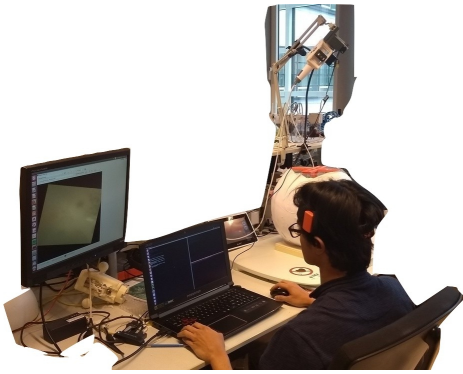

Fig. 14: Experimental setup for Human trials wearing head band.

The overall system for the trial was identical to the standalone experiments conducted previously. The subjects participated in this trials had no prior knowledge about the system. For the setup of the system, the endoscope was placed inside the spherical phantom shown in figure 10. The user is made to wear the head band shown in the figure 14 above. The user will observe an overlaid image stream from the camera on the screen. The user is asked to move his head in certain directions as per the instructions given in Appendix [A]. A small trial run is done at the beginning so that the user gets familiar with the system. There will be 3 trials conducted per user, since we have to test both the sensor fusion algorithms and a comparison with the previous work. From the questionnaire, the performance was evaluated based on confidence, discomfort and how the system was intuitive for the user. Also, the preference of the image output on the screen was evaluated.

III. RESULTS AND DISCUSSION

The results that were obtained from the experiments are shown in this section. They are divided into subsections as same as in II-D.

A. Image Rotation Compensation

The RMSE, mean, standard deviation and the maximum error1 calculated are written in the table for each case below. The results obtained answers one of the sub-questions of this research.

1) Case 1- Free motion of head: The results of the free motion of head from left to right is shown in this section. The error obtained are plotted in the figure 15b below. The mean, standard deviation, RMSE and maximum error calculated for complementary filter, extended kalman filter and the servo motor are shown in table I below.
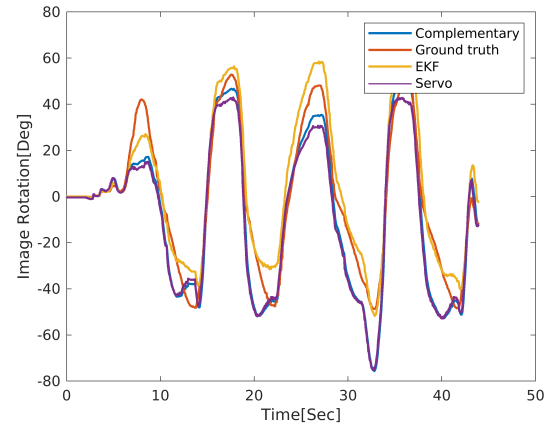
(a) Image rotation compensation output of EKF, complementary filter and previous approach using servo motor compared against ground truth for Case-1
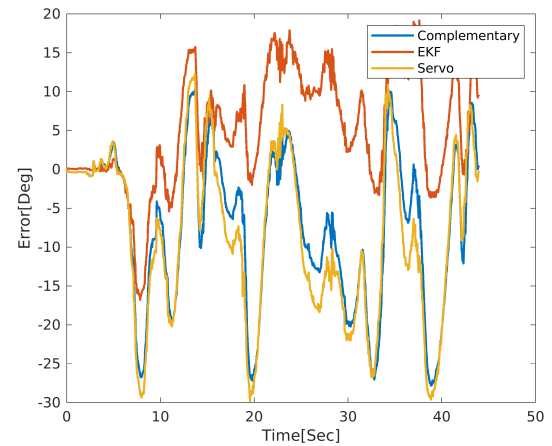
(b) Error plot of servo motor and sensor fusion algorithms.

Fig. 15: Image rotation and Error plot of Case-1

Filter	Mean[°]	Std[°]	RMSE[°]	Max.Error[°]
Complementary	-7.2570	9.7664	12.1639	27.8330
EKF	5.2203	7.4041	9.0567	19.1656
Servo Motor	-8.4710	10.5486	13.5251	29.8160

TABLE I: Measurements obtained from Error plots for Case-1.

From the figure 15 above, sub-figure 15a shows the image

rotation plot and sub-figure 15b shows the error plot of the complementary filter, extended kalman filter. The error of the servo motor was also plotted to compare the results with the previous work. In the figure, the X axis is the time in seconds and the Y axis defines the error in degrees. The standard deviation, RMS value of the sensor fusion algorithms and servo encoder measurement was also calculated and it is shown in the table I above.

From the figure 15, we observe that EKF has a minimum RMSE compared to Complementary filter and Servo motor. This is because the EKF trusts both the measurements from the servo and the image data, hence providing a much better estimate compared to complementary filter which trusts the data from the servo motor more than the image. The RMSE of the complementary is comparitively better than servo because the complementary filter is a low pass filtered output of the servo motor.

2) Case 2- Deflection of the tip: We considered this case to evaluate the image rotation in the finer motion. To validate this, the error obtained were plotted in the figure 16b below. The mean, standard deviation, RMSE and maximum error calculated for complementary filter, EKF and the servo motor are shown in table II below.

| Filter	Mean[°]	Std[°]	RMSE[°]	Max.Error[°]
Complementary	-8.2332	6.9437	10.7683	27.0994
EKF	-5.8579	5.7347	8.1959	20.4571
Servo Motor	-9.2340	7.7547	12.0560	31.0641

TABLE II: Measurements obtained from Error plots for Case-2.

From the figure 16 above, sub-figure 16a shows the image rotation plot and sub-figure 16b shows the error plot of the complementary filter, extended kalman filter. The error of the servo motor was also plotted to compare the results with the previous work. In the figure, the X axis is the time in seconds and the Y axis defines the error in degrees. The standard deviation, RMS value of the sensor fusion algorithms and the servo encoder measurement was also calculated and it is shown in the table II above.

From the table, it is shown that the EKF relatively better compared to Complementary filter and the servo encoder measurement. In the finer motion due to the deflection of the tip, the EKF estimates the image data compared to servo motor hence showing minimum error compared to complementary filter.

3) Case 3- Merged Measurement: In this case, the data were merged and the average of the error obtained by measuring the difference between the ground truth and the servo motor, sensor fusion algorithms were plotted in the figure 17 below. The mean, standard deviation, RMSE and maximum error calculated are shown in table III below and the results are compared with the previous work.

The figure 17 shows the error plot of the complementary filter, extended kalman filter and the servo motor. A random motion from left to right and up to down were measured and the data was merged with the data of the previous two
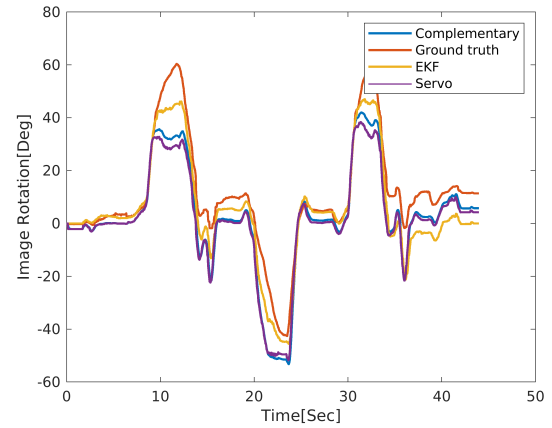
(a) Image rotation compensation output of EKF, complementary filter and previous approach using servo motor compared against ground truth for Case-2
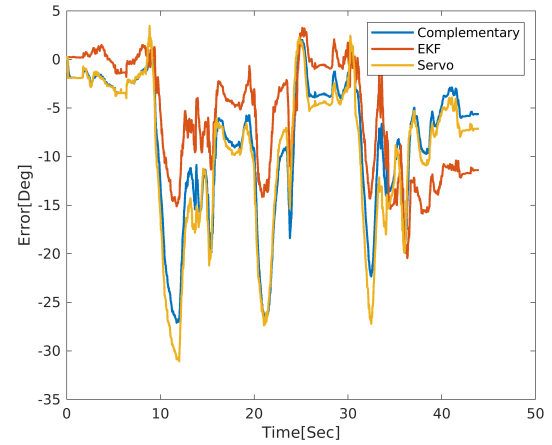
(b) Error plot of servo motor and sensor fusion algorithms.

Fig. 16: Image rotation and Error plot of Case-2.

Filter	Mean[°]	Std[°]	RMSE[°]	Max.Error[°]
Complementary	-4.6156	4.4852	6.4375	14.1531
EKF	0.7713	3.1090	3.1989	9.3895
Servo Motor	-5.1739	4.8243	7.0726	15.9699

TABLE III: Measurements obtained from Error plots for Case-3.

cases. In the figure, the X axis is the time in seconds and the Y axis defines the error in degrees. The standard deviation, RMS value of the sensor fusion algorithms and servo encoder measurement was also calculated and it is shown in the table III above.

For the merged data of the measurement, the two sensor fusion algorithms provide much better results compared to the previous work. But the EKF stands relatively better when compared with complementary filter since the RMSE obtained is low. The image rotation in the finer motion of the complementary filter is still not accurate. These results obtained above answer one of the sub research questions.
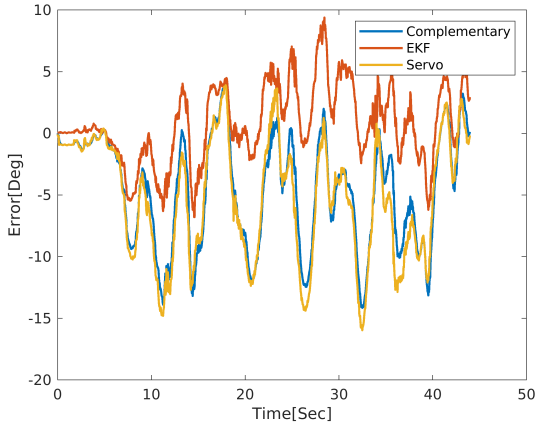
12

Fig. 17: Error plot of Case-3.

B. Tip Movement Validation

The results of the tip movement validation have been discussed in this section below. The hysteresis plots are shown below.
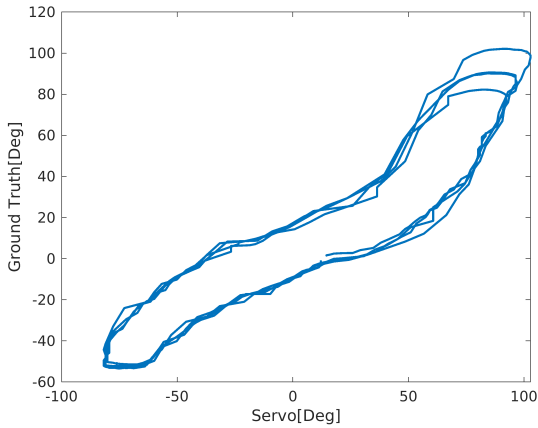

Fig. 18: Hysteresis plot of Servo vs Ground Truth.

In the figure 18 above, the hysteresis behaviour of the system when using the servo encoder measurement as feedback. X axis defined the servo deflection angle q_2 and Y axis was the angle obtained from the ground truth (NDI). In figure 19, the hysteresis behaviour of the system using complementary filter is shown. Here, the X axis is the fused angle obtained and Y axis is the angle obtained from ground truth. Finally in figure 20, the hysteresis behaviour of the system using EKF is shown. The X axis is the fused angle and Y axis is the angle obtained from the ground truth.

For the behaviour of the system when using servo encoder measurement, the percentage of the ground truth hysteresis plot was 14%. Non-linearities are present due to the non-centered cable mechanism of the flexible endoscope. Also, only position control is possible using the servo motors used in this project.[5].

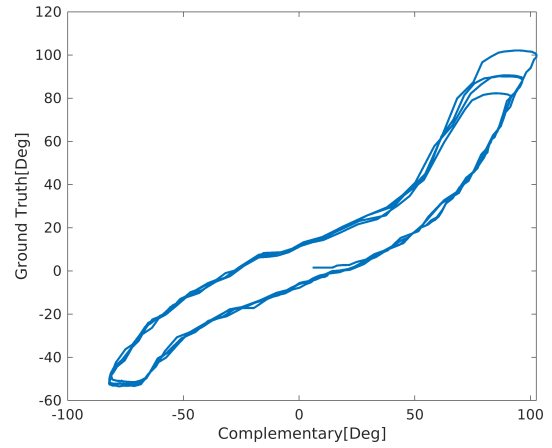For obtaining the fused angle, servo deflection angle q_2

Fig. 19: Hysteresis plot of Complementary filter vs Ground Truth.

was merged with the angular velocity obtained from the translation along the y-axis of the output image. The percentage was calculated to be 8%. The hysteresis behaviour of the complementary filter is reduced since the complementary filter trusts both the incoming measurements compared to the previous case when only servo encoder measurement is used as feedback.
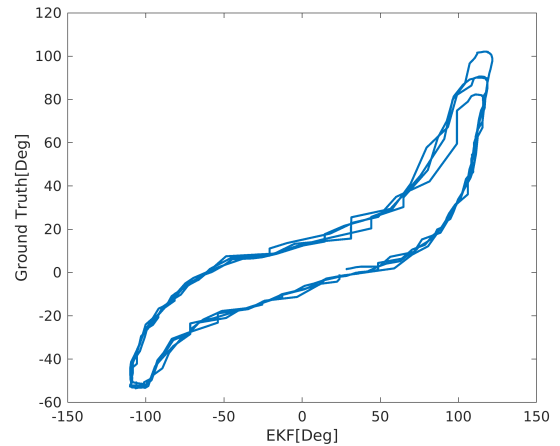

Fig. 20: Hysteresis plot of Extended Kalman Filter vs Ground Truth.

The angle obtained from the motor q_2 was fused with the angular velocity obtained from the translation along the y-axis of the output image. After the calculation for percentage of hysteresis, it was found out that the EKF had 11%.

Comparing the results from the cases above, it was observed that there was a significant decrease in the hysteresis percentage when two sensor fusion algorithms were used compared to the servo motor. This is because the EKF and the complementary filter uses the image data in compensating for non-linearities along the deflection axis. However, it was noticed that EKF was trusting the servo

13

encoder measurement compared to the image data. Hence the results of EKF are almost similar to the case of servo encoder measurement. The complementary filter trusts both the measurements resulting in low hysteresis percentage. Hence we can use the complementary filter to compensate for the non-linearities in the actuation since we can fine tune the values of the complementary filter compared to EKF.

C. Human Trials for Performance of the System

Human trials were conducted on the subjects who were untrained in interventional endoscopy procedures. The trials conducted does not include time required for training and time taken to complete the task, since we are interested only in the output of the image on the screen. The instructions for the trials are explained in Appendix [A] and the responses of the questionnaire (N=12) are discussed below.

1) Questionnaire results: The performance was evaluated based on the confidence, intuitiveness, discomfort felt during the experiment and the preference of the image output on the screen. The results obtained from the questionnaire are shown in the charts below. They are separated into 3 methods. Here, Method 1 refers to the image rotation compensation based on servo encoder measurement. Method 2 refers to the image rotation compensation based on complementary filter and Method 3 refers to the image rotation compensation based on Extended kalman filter (EKF). A stacked bar chart representing the responses from the subjects for confidence, discomfort and intuitiveness is shown in figure 21 below. A pie chart describing the preference of the image rotation compensation is shown in figure 22 below.
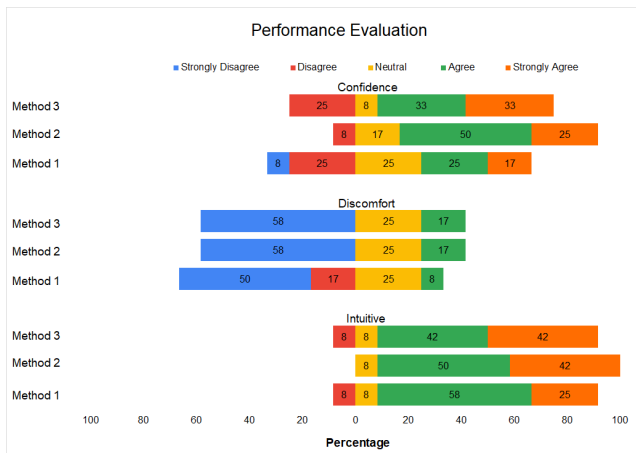

Fig. 21: Performance evaluation of the subjects

From figure 21, 8% of the subjects believed that Method 1 and Method 3 were not intuitive. 17% of the subjects experienced some discomfort when they were performing Method 2 and Method 3. Evaluating all the responses from figure 21, we can observe that Method 2 is preferred over Method 3 and Method 1. These results are backed up by the preference of choosing the output image rotation compensation on the screen shown in figure 22. Only 8% agreed that they would prefer Method 1 over other two methods. From
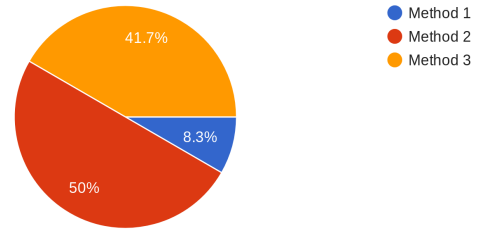

Fig. 22: Pie chart representing image rotation compensation preference of subjects.

the observations of the subjects, Method 2 had a smooth transition of image on the screen when compared to other two methods. 91.7% preferred the two sensor fusion algorithms, where 50% preferred the complementary filter and the rest opted for EKF. These results answer one of the sub research questions mentioned in section I.

IV. CONCLUSIONS

In this paper, the sensor fusion technique for head motion controlled endoscope camera system has been successfully realized. The new Ambu scope was mounted on the new design of the robot handle. Several validation tests were conducted to evaluate the accuracy of the image rotation compensation and to compensate for hysteresis compensation. Human trials were evaluated for preference of the image rotation compensation after applying sensor fusion algorithms. The results obtained were compared with previous work.

From the accuracy test of the image rotation compensation, we can conclude that the EKF is comparitely better sensor fusion algorithm than complementary filter. While the methods were also tested for compensating of hysteresis behavior in the actuation of motors, the hysteresis percentage of complementary was relatively low compared to EKF. From the responses of human trials conducted to measure the overall performance of the system, the complementary filter is preferred over EKF. This causes a trade-off between choosing the sensor fusion algorithms. If complementary filter is chosen, then the values of α and $d\tau$ must be fine tuned to obtain better results in finer motion. If EKF is chosen, then the values of Q matrix must be fine tuned to a higher value to obtain better results for compensating hysteresis behavior.

To sum up, the main goal of this paper was how can we improve the performance of image rotation compensation and remove non-linearities in the actuation of the head motion controlled endoscope system. The goal was achieved and the results obtained above clearly show that the sensor fusion algorithms can be used for improving the performance of the image rotation compensation and compensate for non-linearities in the actuation of the motors.

REFERENCES

[1] H. Hansen, R. Petersen, "Video-assisted thoracoscopic lobectomy using a standardized three-port anterior approach - The Copenhagen experience", Annals of Cardiothoracic Surgery, March 2012.

[2] R. Reilink, G. de Bruin, M. Franken, S. Misra, S. Stramigioli and M. A. Mariani, "Endoscopic Camera Control by Head Movements for Thoracic Surgery", IEEE RAS and EMBS International Conference on Biomedical Robotics and Biomechatronics, pp. 515-520, September 2010.

[3] J. M. Sackier and Y. Wang, "Robotically assisted laparoscopic surgery," Surgical Endoscopy, vol. 8, pp. 63–66, January 1994.

[4] Prosurgics, "Freehand, a laparoscopic camera controller,"http://www.freehandsurgeon.com/, Accessed 04 Jan 2010.

[5] Y. X. Mak, "Head Motion Controlled Endoscopic Camera Manipulation using Inertial Motion Sensor and Mixed Reality Headset", M.S. thesis, Dept. Elec. Eng., Twente Univ., Enschede, Netherlands, December 2018.

[6] H. T. Tevaearai, F. S. Xavier, M. Mueller and, P. Ruchat, and L. K. von Segesser, "Advantages of a modified gastroscope for video-assisted internal mammary artery harvesting," Annals of Thoracic Surgery, pp. 872–873, March 1999.

[7] T. Yokoyama, R. Toda, R. Tomioka, and H. Aizawa, "Thoracoscopy: assessment of a physician service and comparison of a flexible bronchoscope used as a thoracoscope with a rigid thoracoscope," Thorax, vol. 43, pp. 327–332, April 1988.

[8] K. J. R. Selman, "Development and validation of a position aiding system for inertial motion capture using Microsoft HoloLens", M.S. thesis, Dept. Elec. Eng., Twente Univ., Enschede, Netherlands, September 2017.

[9] V. S. Raghavan, "A Sensor Data Fusion Algorithm for Human Motion Estimation", M.S. thesis, Dept. Mech. Mari. and Mat. Eng., Delft Univ., Delft, Netherlands, October 2016.

[10] P. Gui, L. Tang, S. Mukhopadhyay, "MEMS Based IMU for Tilting Measurement: Comparison of Complementary and Kalman Filter Based Data Fusion", IEEE 10th Conference on Industrial Electronics and Applications(ICIEA), pp. 2004-2009, June 2015.

[11] T. Moore, D. Stouch, "A Generalized Extended Kalman Filter Implementation for the Robot Operating System", pp. 335-348, January 2016.

[12] G. Welch, G. Bishop, "An Introduction to the Kalman Filter", January 2006.

[13] S. Colton, "The Balance Filter: A Simple Solution for Integrating Accelerometer and Gyroscope Measurements for a Balancing Platform", June 2007.

[14] web.mst.edu,"Explanation of Hysteresis calculation.doc", https://web.mst.edu/cottrell/ME240/Resources/Calibration/ExplanationofHysteresiscalculation.doc.

[15] M. W. Tao, J. Bai, P. Kohli and S. Paris, "SimpleFlow: A Non-iterative, Sublinear Optical Flow Algorithm", Computer Graphics Forum, vol. 31, pp. 345-353, May 2012.

[16] "Video-Assisted Thoracic Surgery (VATS)," Cleveland Clinic. [Online]. Available: https://my.clevelandclinic.org/health/treatments/17617-video-assisted-thoracic-surgery-vats. [Accessed: 06-Nov-2019].

15

3 Conclusion

A sensor fusion technique for head motion controlled endoscope camera system has been successfully realized in this project. The new Ambu scope was mounted on the new design of the robot handle. Several validation tests were conducted to evaluate the accuracy of the image rotation compensation and to compensate for hysteresis compensation. Human trials were evaluated for preference of the image rotation compensation after applying sensor fusion algorithms. The research question mentioned below answers the results obtained in this study. Further conclusions were drawn in comparison with previous work.

How can we improve the performance of the overall system after compensating for image rotation compensation and non-linearities in the actuation of the head motion controlled system?

From the accuracy test conducted for image rotation compensation, we can conclude that EKF is comparitevely better sensor fusion algorithm compared to complementary filter due to low RMSE value obtained. The results also showed improvement when compared to the previous method. The hysteresis compensation was done on the deflection axis and from the results we can conclude that the hysteresis percentage of complementary filter is relatively lower compared to EKF and servo encoder measurement. The human trials were conducted for evaluating the performance of the overall system after applying sensor fusion technique and the results showed that the complementary filter was preferred over EKF and servo encoder measurement. Considering the preference of image output on the screen, 91.7% subjects preferred the two sensor fusion algorithm compared to the servo encoder measurement. From the results obtained above, there is a trade-off between choosing a better sensor fusion algorithm. If complementary filter was chosen, then the values of α and $d\tau$ must be fine tuned to obtain better results in the finer motion. If EKF was chosen, then the values of Q matrix must be fine tuned to a higher value. From these results, we can finally conclude that a sensor fusion technique can be used for improving the overall performance of the head motion controlled endoscope camera system.

Moreover, a sensor fusion technique not only resolves the limitations related to the visual feedback-system during VATS but also increases the accuracy of the image output on the screen as discussed above. This allows the clinicians to work more efficiently during the operations. Due to the compensation of the hysteresis by sensor fusion technique, the accuracy of the up and down head motion is increased and this makes the overall system more intuitve and easy to use.

3.1 Limitations and Future work

The limitations of the system and the possible future work are discussed below.

3.1.1 Limitations

- The endoscope camera image quality and the resolution are restricted for optical flow algorithm. Due to this the measurements of image which are used for sensor fusion algorithm are affected. An endoscope with better and high image quality must be chosen to obtain better results.

3.1.2 Recommendations for Future Work

- For compensating for hysteresis behavior in the deflection axis, a basic feedback loop can be designed by using the output from the complementary filter. This is shown in the figure 3.1 below, where CF is the complementary filter, e refers to the error and y refers to the output.
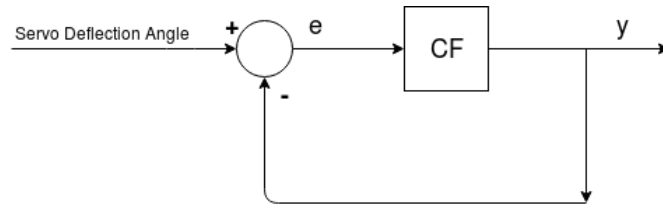
Figure 3.1: Basic feedback loop for compensating Hysteresis

- A heart rate sensor can be used to obtain the data from the user and display the output on the screen of hololens, giving clinicians a more possibility at looking persons vitals during the operation.

A Head Scope Performance experiment documents

A.1   Instruction Manual for Participants

A.1.1   Introduction

First of all I would like to thank you for participating in this research.This document has been made as an instruction manual to prepare for the experiment. If you have any questions after reading this manual please ask them.

The goal of this research to test the accuracy and performance of the overall system after implementing a sensor fusion algorithm in the system. During this experiments, the image rotation compensation of the two sensor fusion algorithms are compared with the previous work. After the end of the experiment, a questionnaire will be followed. This whole experiment would take around 30 minutes.

A.1.2   Instructions

During the test, you will be wearing a headband used to control the robot arm. The footswitch pedal enables you to switch on and off the control of the robot arm. If you move your head up and down, the camera moves up and down. If you move your head left and right, the camera moves left and right. For evaluating the goal of the research, you will have to move your head according to the steps below.

1. The black mark in the figure A.1 below is the starting point of the task.

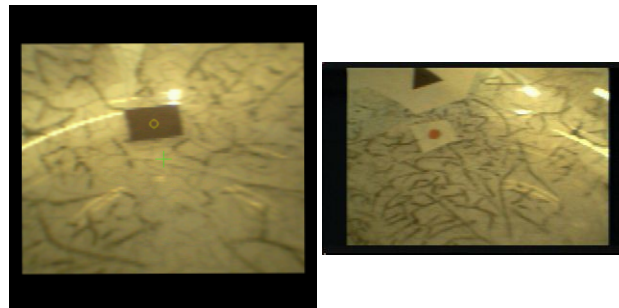2. Move your head to the left and notice a red mark in figure A.1.

Figure A.1: Screenshot of Black (left) and Red (right) mark inside the dome.

3. After you observe the red mark, come to the center and then move your head to the right to see the green mark in figure A.2.
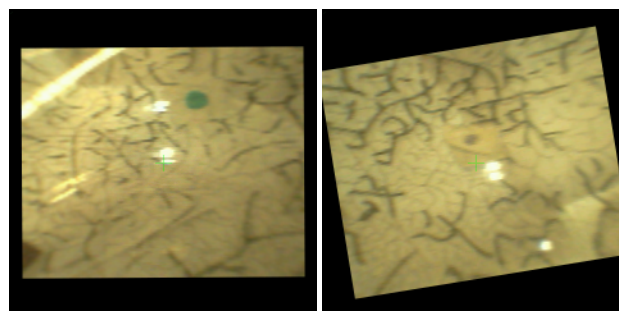

Figure A.2: Screenshot of the Green (left) and Blue (right) mark inside the dome.

4. After noticing the green mark, come back to the starting point and move your head up to see a blue mark in figure A.2.

5. After noticing this point, please come back to the starting point by moving your head down.

During this head movement, the image output will be put up on the screen. Please watch them closely. You will be conducting the experiments thrice to test 3 methods. If you feel uncomfortable at any point, please let us know. You will be getting a test run before the experiments to get comfortable using the system. If you have any questions during the test, feel free to ask them. Try to perform the test as accurate as possible. If you have any specific questions, feel free to ask them. Also try not to get distracted during the experiment. The questionnaire will be followed after the end of the test.

A.2 Questionnaire and Consent form

Questionnaire- Experimental Setup

Informed Consent

1. **I have read and understood the Instructions for experiment 'Head Scope Performance'. I had the opportunity to ask question about it and any questions that i have been asked have been answered to my satisfaction. I consent voluntarily to participate in this research. ***
   Check all that apply.

   ☐ Agree

Personal Data

2. **Name ***

   _____

3. **Email ***

   _____

Head Scope Performance

4. **Method 1 ***
   Mark only one oval per row.

	Strongly Disagree	Disagree	Neutral	Agree	Strongly Agree
System was intuitive	⬭	⬭	⬭	⬭	⬭
System was easy to use	⬭	⬭	⬭	⬭	⬭
I felt discomfort while using the system.	⬭	⬭	⬭	⬭	⬭
I was confident while using the head motion controlled endoscope system.	⬭	⬭	⬭	⬭	⬭

5. **Method 2** *

Mark only one oval per row.

	Strongly Disagree	Disagree	Neutral	Agree	Strongly Agree
System was intuitive	⬭	⬭	⬭	⬭	⬭
System was easy to use	⬭	⬭	⬭	⬭	⬭
I felt discomfort while using the system.	⬭	⬭	⬭	⬭	⬭
I was confident while using the head motion controlled endoscope system.	⬭	⬭	⬭	⬭	⬭

6. **Method 3** *

Mark only one oval per row.

	Strongly Disagree	Disagree	Neutral	Agree	Strongly Agree
System was intuitive	⬭	⬭	⬭	⬭	⬭
System was easy to use	⬭	⬭	⬭	⬭	⬭
I felt discomfort while using the system.	⬭	⬭	⬭	⬭	⬭
I was confident while using the head motion controlled endoscope system.	⬭	⬭	⬭	⬭	⬭

7. **Which method do you prefer for image rotation compensation?** *

Mark only one oval.

◯ Method 1

◯ Method 2

◯ Method 3

Bibliography

Gui, P., L. Tang and S. Mukhopadhyay (2015), MEMS based IMU for tilting measurement: Comparison of complementary and kalman filter based data fusion, pp. 2004–2009, doi: 10.1109/ICIEA.2015.7334442.

Hansen, H. J. and R. H. Petersen (2012), Video-assisted thoracoscopic lobectomy using a standardized three-port anterior approach - The Copenhagen experience, **vol. 1**, no.1, pp. 70–76, ISSN 2225-319X, doi:10.3978/j.issn.2225-319X.2012.04.15, 23977470[pmid]. https://www.ncbi.nlm.nih.gov/pubmed/23977470

Mak, Y. (2018), Head Motion Controlled Endoscopic Camera Manipulation using Inertial Motion Sensor and Mixed Reality Headset.

Minor, A., J. Villalobos, R. Ordorica-Flores and D. Espinoza (2008), Postural mechatronic assistant for laparoscopic solo surgery (PMASS), *Surgical endoscopy*, **vol. 23**, pp. 663–7, doi:10.1007/s00464-008-9982-0.

Raghavan, V. (2016), A Sensor Data Fusion Algorithm for Human Motion Estimation.

Reilink, R., G. de Bruin, M. Franken, M. A. Mariani, S. Misra and S. Stramigioli (2010), Endoscopic camera control by head movements for thoracic surgery, in *2010 3rd IEEE RAS EMBS International Conference on Biomedical Robotics and Biomechatronics*, pp. 510–515, doi:10.1109/BIOROB.2010.5627043.

Sackier, J. M. and Y. Wang (1994), Robotically assisted laparoscopic surgery, **vol. 8**, no.1, pp. 63–66, ISSN 1432-2218, doi:10.1007/BF02909496. https://doi.org/10.1007/BF02909496

Selman, K. (2017), Development and validation of a position aiding system for inertial motion capture using Microsoft HoloLens.